Phase Transition in Warm Nuclear Matter with Alternative Derivative Coupling Models

M. Malheiro [1,2] [*], A. Delfino [1] [†] and C. T. Coelho[1]

[1] Instituto de Física, Universidade Federal Fluminense,
24210-340, Niterói, R. J., Brasil
[2] Department of Physics, University of Maryland,
College Park, Maryland 20742-4111, USA

February 9, 2008

Abstract : An analysis is performed of the liquid-gas phase transition of nuclear matter obtained from different versions of scalar derivate coupling suggested by Zimanyi and Moszkowski (ZM) and the results are compared with those obtained from the Walecka model. We present the phase diagram for the models and one of them, the ZM3 model, has the lowest critical temperature $T_c = 13.6$ MeV with the lowest critical density $\rho_c = 0.037$ fm^{-3} and pressure $p_c = 0.157$ MeV fm^{-3}. These results are in accord with recent observations from energetic heavy-ion collisions, which suggest a small liquid-gas phase region.

PACS # 21.65.+f, 12.40.Yx, 25.75.+r

[*]Partially supported by CAPES of Brasil
[†]Partially supported by CNPq of Brasil

1 Introduction

Nowadays, the study of the liquid-gas phase transition, which may occur in the warm and dilute matter produced in energetic heavy-ion collisions, is one of the interesting problems in nuclear physics [1]. This idea of that nuclear systems may show up a critical behavior has initiated more than ten years ago with the observation by the Purdue-Fermilab group of asymptotic fragment charge distributions exhibiting a power law [2]. This interest increased recently with the attempt by the EOS Collaboration to extract critical exponents of fragmenting nuclear systems produced in the collision of 1 GeV/nucleon Au nuclei with a carbon target [3], and with the extraction by ALADIN/LAND Collaboration of a caloric curve resulting from the fragmentation of the quasiprojectile formed in the collision Au + Au at 600 MeV/nucleon exhibiting a behavior expected for a first order liquid-gas phase transition [4].

At the time where the search for signals of liquid-gas nuclear phase transition are taking place, it is important to have ready the theoretical phase-transition predictions for a broad class of different hadronic models. The main ingredient in this analysis is the nuclear matter equation of state (EOS) at finite temperature. The success of relativistic mean-field theories describing cold nuclear matter and bulk nuclear properties throughout the periodic table, suggests the use of a relativistic mean-field EOS. Moreover, the mean-field approximation is known to be thermodinamicaly consistent: the relevant thermodynamic identities are all satisfied [5], [6].

Recently variants of Zimanyi and Moszkowski (ZM) model [7] were implemented and applied by us to dense and cold nuclear matter [8], [9]. The usual ZM model, also referred to in the literature as the Derivative Scalar Coupling model (DSC), consists of derivative coupling between nucleons and scalar mesons σ. The model has been extended to include a non-linear interaction between the nucleon and the vector meson ω. Two types of this interaction were employed and the resulting models were denoted ZM2 and ZM3. These models were designed to cure the defects of the Walecka model [10], namely the low effective nucleon mass and the large incompressibility of nuclear matter. Each one of them is very simple since they have only two free parameters, the scalar (vector) coupling constants C_σ^2 (C_ω^2), adjusted to reproduce the binding energy (E_b) of the nuclear matter at $\rho = \rho_0$. The degrees of freedom are baryon fields (ψ), scalar meson fields (σ), and vector meson fields (ω).

In all ZM models, there are non-linear interaction terms which in a approximate way incorporate the effect of many-body forces. After an appropriate rescaling of the Lagrangians, these models can be understood as generalizations of the Walecka Model where the scalar and vector meson couplings become effectively density-dependent [11]. This fact underlies the recent approach, known as relativistic density-dependent Hartree-Fock [12],

[13], [14] which describes finite nuclei and nuclear matter saturation properties using coupling constants that are fitted, at each density value, to the relativistic Brueckner-Hartree-Fock self-energy terms. The good agreement obtained for the ground state properties of spherical nuclei lends support to such density-dependent coupling constants. Recently, it was shown that chiral symmetry restoration requires the meson-nucleon coupling to be density dependent [15].

The aim of this paper is to extend our study to include temperature effects, and to perform an analysis of the liquid-gas phase transition of the warm nuclear matter obtained on these three ZM models and compare to the linear Walecka (W) model [16]. We present the effective nucleon mass, energy per nucleon, pressure, and entropy density as a function of the baryonic density at different temperatures. We show the isotherms, construct the phase diagram with the phase coexistence boundary, and present the critical and flash temperatures for the models. The usual ZM model has already been applied to investigate some thermodynamic properties of nuclear matter [17] and recently, the modified versions have been used in order to study the density and temperature dependence of hadron masses [18].

The outline of the paper is as follows: in the next section we present the EOS at finite temperature. Section 3 includes our results and discussion of the thermodynamic properties of nuclear matter. Finally, we summarize.

2 The nuclear matter EOS at finite temperature

Since the models we are dealing with were discussed in detail in references [7], [8], [9], here we will only present the Lagrangian obtained after rescaling the nucleon field as $\psi \rightarrow m^{*1/2}\psi$ for all ZM models and making the rescaling $\omega_\mu \rightarrow m^*\omega_\mu$ for ZM2 and ZM3 models:

$$\begin{aligned}\mathcal{L}_R &= \bar{\psi} i\gamma_\mu\partial^\mu\psi + m^{*^\alpha}\left(-g_\omega\bar{\psi}\gamma_\mu\psi\omega^\mu - \frac{1}{4}F^{\mu\nu}F_{\mu\nu} + \frac{1}{2}m_\omega^2\omega_\mu\omega^\mu\right) \\ &- \bar{\psi}(M - m^{*^\beta}g_\sigma\sigma)\psi + \frac{1}{2}(\partial_\mu\sigma\partial^\mu\sigma - m_\sigma^2\sigma^2), \end{aligned} \quad (1)$$

where α and β have the following values for the different models, $W : \alpha = 0, \beta = 0$; $ZM : \alpha = 0, \beta = 1$; $ZM2 : \alpha = 1, \beta = 1$; $ZM3 : \alpha = 2, \beta = 1$; and $m^* = (1 + g_\sigma\sigma/M)^{-1}$ in all three cases, M is the bare nucleon mass and $F_{\mu\nu} = \partial_\mu\omega_\nu - \partial_\nu\omega_\mu$.

When the meson fields are replaced by the constant classical fields σ_o and ω_o we arrive at the mean-field approximation, with the equation of motion for the nucleon:

$$[i\gamma_\mu\partial^\mu - (M - m^{*^\beta}g_\sigma\sigma) - m^{*^\alpha}g_\omega\gamma_\mu\omega^\mu]\psi = 0, \quad (2)$$

where the effective nucleon mass M^* is given by $M^* = M - m^{*\beta} g_\sigma \sigma$. In the case of ZM models where $\beta = 1$ we can identify $m^* = M^*/M = (1 + g_\sigma \sigma/M)^{-1}$.

The expression for the energy density and pressure at a given temperature T can be found as usual by the average of the energy-momentum tensor,

$$\mathcal{E} = \frac{C_\omega^2}{2M^2} m^{*^\alpha} \rho^2 + \frac{M^4}{2C_\sigma^2} \left(\frac{1 - m^*}{m^{*\beta}} \right)^2 + \frac{\gamma}{(2\pi)^3} \int d^3k \, E^*(k)(n_k + \bar{n}_k), \tag{3}$$

$$p = \frac{C_\omega^2}{2M^2} m^{*^\alpha} \rho^2 - \frac{M^4}{2C_\sigma^2} \left(\frac{1 - m^*}{m^{*^\beta}} \right)^2 + \frac{1}{3} \frac{\gamma}{(2\pi)^3} \int d^3k \, \frac{k^2}{E^*(k)} (n_k + \bar{n}_k). \tag{4}$$

Thus we obtain the entropy density:

$$\begin{aligned} s &= \frac{1}{T} \left[\frac{C_\omega^2}{M^2} m^{*\alpha} \rho^2 + \frac{\gamma}{(2\pi)^3} \int d^3k \, E^*(k)(n_k + \bar{n}_k) \right] \\ &+ \frac{1}{3T} \frac{\gamma}{(2\pi)^3} \int d^3k \, \frac{k^2}{E^*(k)} (n_k + \bar{n}_k) - \frac{\mu\rho}{T}, \end{aligned} \tag{5}$$

where γ is the degeneracy factor ($\gamma = 4$ for nuclear matter and $\gamma = 2$ for pure neutron matter), n_k and $\bar{n}_k$ stand for the Fermi-Dirac distribution for baryons and antibaryons respectively, with arguments $(E^* - \nu)/T$, $E^*(k)$ is given by $E^*(k) = (k^2 + M^{*2})^{\frac{1}{2}}$. An effective chemical potential which preserves the number of baryons and antibaryons in the ensemble is defined by $\nu = \mu - V$, with μ is the thermodynamical chemical potential. We have introduced $C_\sigma^2 = g_\sigma^2 M^2/m_\sigma^2$ and $C_\omega^2 = g_\omega^2 M^2/m_\omega^2$.

The effective mass is obtained explicitly through the minimization of $\mathcal{E}$ with respect to m^* and must satisfied the self-consistent equation,

$$1 - m^* - \frac{\gamma C_\sigma^2}{2\pi^2} m^{*^{3\beta+1}} \int \frac{x^2 dx}{\sqrt{x^2 + m^{*^2}}} (n_x + \bar{n}_x) - \frac{\alpha}{2} \frac{C_\sigma^2 C_\omega^2}{M^6} m^{*^{\alpha+2\beta}} \rho^2 = 0 \tag{6}$$

where we have used the dimensionless variable $x = \frac{k}{M}$.

The energy density can be fitted to the nuclear matter ground state energy and saturation density ρ_o at zero temperature to obtain the different coupling constants for the models. They are presented in table 1 together with the nuclear matter incompressibility that at $T = 0$ is given by:

$$K = 9\rho_o^2 \frac{\partial^2}{\partial \rho^2} (\frac{\mathcal{E}}{\rho})|_{\rho=\rho_o} = 9\rho_o \frac{\partial^2 \mathcal{E}}{\partial \rho^2}|_{\rho=\rho_o}. \tag{7}$$

To compute the thermodynamic functions, one first chooses T and ν. The self-consistency condition in eq.(6) is then solved to determine M^* (note that there may be several solutions for fixed T and ν). These solutions specify the distribution functions n_k and $\bar{n}_k$, and the remaining integrals in Eqs. (3), (4) and (5) can then be evaluated directly.

3 Results and Discussion

In Fig. 1 we show M^* as a function of T at zero density. In this regime, the vector field proportional to ρ vanishes, and so the three ZM models differ only in having different values of their scalar coupling constants C_σ^2. The ZM and the Walecka model coincide in the lower temperature region $T \leq 120$ MeV and ZM3 model stay together up to $T \sim 160$ MeV. However, at higher temperature the models separate quite clearly, with the effective nucleon mass in the ZM models dropping more slowly than that in the Walecka Model. This means that the sigma field (the source for the scalar density), increases more slowly with temperature in ZM models because of the inclusion of non linear interactions which are absent in the Walecka Model. As a result, the attraction is stronger in the Walecka model favouring the formation of nucleon-antinucleon pairs at high temperature. Moreover, none of the proposed ZM models is able to present a first order phase transition at $\rho = 0$, $T \neq 0$. This is in contrast to the Walecka model, which has such a phase transition at $T \sim 185$ MeV [19].

In Fig. 2 we show the behavior of the effective nucleon mass with density at different temperatures for all the models. For low temperatures the results are not so different from those obtained at zero temperature, showing that in this regime the density dependence is more important than the temperature dependence. As temperature is raised, M^* first increases and then decreases more slowly for ZM models than Walecka model at $T = 200$ MeV. Within ZM models, this decrease is more pronounced in ZM3, but is even smaller compared to Walecka model where the effective mass goes down very fast. In short, the effect of the temperature on the effective nucleon mass in the ZM models is not so pronounced as in the case of Walecka Model, and can be seen only for densities below the normal density.

We present the energy per nucleon as a function of the density at various temperatures in Fig. 3 . As the temperature increases the nuclear matter becomes less bound and the the saturation curve around the equilibrium point in the ZM models is flatter than that in the Walecka model. This indicates that the nuclear matter EOS in ZM models is softer compared to the obtained in the Walecka Model, even at finite temperature. We can also conclude that the incompressibility of nuclear matter decreases when the temperature increases. This can be seen more clearly in Fig. 4 where we show the pressure-density isotherms of nuclear matter at different temperatures. Since the incompressibility K is related to $\partial p/\partial\rho$ (calculated at the equilibrium point where the pressure vanishes), we see directly that when the temperature increases K decreases, and among the ZM models, the ZM3 model always gives the softest EOS for a fixed temperature.

The isotherms exhibit a typical Van der Waals like interaction where a liquid and gaseous phases coexist, with an unphysical region in the midle of each isotherm that gets

smaller as the temperature increases. For very small temperatures the isotherms manifest the following behavior: for very low density the pressure increases with temperature as for as a ideal gas, $p \sim \rho k_b T$. It decreases subsequently because of the attractive interaction of the sigma field, and finally increases as a consequence of the repulsion coming from the vector meson which dominates at high density. When temperature increases, the term $\rho k_b T$ becomes more important and the local minimum in the pressure is less pronounced and disappears when the temperature is equal to the critical T_c. At this temperature, the unphysical region disappears and an inflection point appears in the isotherm, as we show in the Fig.4 for each model. The p-ρ isotherms in the ZM models have a shallower and more even valley than the corresponding ones in the Walecka Model, and this is more noticeable in ZM3 model. In table 2 we list the critical temperature T_c, density ρ_c and pressure p_c given by the ZM and Walecka models. The ZM3 model presents the lowest $T_c = 13.6$ MeV, density $\rho_c = 0.037$ fm^{-3} and pressure $p_c = 0.157$ MeV fm^{-3}.

The phase coexistence boundary is determined by Gibbs's criteria, namely, that the liquid and gas phases have equal temperatures (thermal equilibrium), chemical potentials (chemical equilibrium), and pressures (hydrostatic equilibrium). We present in Fig.5 the phase diagram Txρ of the models. Below the coexistence curve of each one, the equilibrium state is a mixture of gas and liquid. This region is bigger in the Walecka model. In fact, if we include nonlinear terms in this model, this region becames smaller and the critical temperature goes down to $T_c = 14.2$ MeV [5]. The ZM3 model, where the non-linearity of the coupling between the vector field to the nucleon is strongest, presents the smallest phase coexistence region comparing to the other models.

As we have already pointed out, the nuclear matter incompressibility K decreases when the temperature increases. So, we will have a temperature where the incompressibility K calculated at the equilibrium point vanishes. This temperature is known as the flash temperature $T = T_f$, $\frac{\partial p}{\partial \rho}|_{T_f} = p(\rho_f, T_f) = 0$. It represents the highest temperature at which a self-bound system can exist in hydrostatic equilibrium ($p = 0$). Above this temperature the warm nuclear matter is unbound and starts expanding. We present in Fig. 6 the pressure as a function of baryon density at the flash temperature for the models. This temperature in MeV is 14.1, 12.9, 12.2 and 11.0 for the Walecka, ZM, ZM2 and ZM3 models respectively. Again, the ZM3 model has the smallest flash temperature. As expected, all of these temperatures are lower than the critical ones, because, as Fig.4 shows, at the critical temperature the pressure is already positive and the system is expanding.

Finally, we present in Fig.7 the entropy density as a function of the density at different temperatures. For high temperatures ($T = 200$ MeV), we see an increase in the entropy density with the density for all the models. This happens even at very low densities, and manifests what we have already pointed out when we have discussed the behavior of the effective nucleon mass with the temperature at zero density. This decrease of M^* or

increase of the entropy density with increasing temperature, which is more pronounced in the Walecka and ZM3 models, resembles a phase transition. At high temperature and low density the system becomes a dilute gas of baryons in a sea of baryons-antibaryons.

In summary, we have presented the thermodynamic properties of nuclear matter in three different versions of the ZM model. We have shown how the effective nucleon mass M^*, energy per nucleon, pressure, and entropy behaves as a function of the density for different temperatures. As in the zero temperature case, all the ZM models give a softer EOS of nuclear matter at finite temperature than the Walecka model. Among the three ZM models, ZM3 is the softest. Unlike the Walecka Model the ZM models do not exhibit a phase transition for finite temperature at zero density. We studied the liquid-gas phase transition, and concluded that the ZM3 model presents the smallest phase coexistence region with the lowest critical temperature, density and pressure. The incompressiblity decreases with the increasing temperature, and vanishes when $T = T_{flash}$. Again, the ZM3 model has the smallest flash temperature. The experimental results investigating this warm and dilute matter produced in energetic heavy-ion collisions suggest a small liquid-gas phase region and a low critical temperature [4], [1]. This suggests that the good description of nuclear matter properties obtained in the ZM3 model at zero temperature remains, even at finite temperature, and makes the ZM3 model the most suitable of all models used.

One of us (MM) would like to thank Dr. D. R. Phillips for careful reading of the manuscript, the Maryland TQHN Group supported by the U.S. Depto. of Energy for their hospitality during his extended stay, and gratefully the CAPES of the Brazilian Governement for the financial support which made this visit possible.

References

[1] T. Li et al, Phys. Rev C49, 1630 (1994) (Michigan National Superconducting Cyclotron Laboratory; They extracted a critical value for the slope parameter that converges for $T_c = 13.1 \pm 0.6$ MeV)

[2] J. E. Finn et *al*, Phys. Rev. Lett. **49**, 1321 (1982); Phys. Lett. **B118**, 458 (1982); M. Mahi et *al*, Phys. Rev. Lett. **60**, 1936 (1988)

[3] J. B. Elliot et *al*, Phys. Rev. **C49**, 3185 (1994); M. L. Gilkes et *al*, Phys. Rev. Lett **73**, 1590 (1994)

[4] J. Pochodzalla et *al*, Phys. Rev. Lett. **75**, 1040 (1995) from ALADIN/LAND Collaboration; International Nuclear Physics Conference **(INPC'95)**, Beijing-China, August 1995, (Book of Abstract, section Invited Talks, pg. I-16)

[5] R. J. Furnstahl and B. D. Serot, Phys. Rev. **C41**, 262 (1990).

[6] H. Muller and B. D. Serot, Phys. Rev. **C52**, 2072 (1995)

[7] J. Zimanyi and S. A. Moszkowski, Phys. Rev. **C42**, 1416 (1990).

[8] A. Delfino, C. T. Coelho and M. Malheiro, Phys. Lett. **B345**, 361 (1995).

[9] A. Delfino, C. T. Coelho and M. Malheiro, Phys. Rev. **C51**, 2188 (1995).

[10] B. D. Serot and J. D. Walecka, Adv. in Nucl. Phys. **16** (1986).

[11] A. Delfino, M. Chiapparini, M. Malheiro, L. V. Belvedere and A. O. Gattone, Zeits. fur Phys.**A** (In press), nucl-th/9602004.

[12] Hua-lin Shi, Bao-qiu Chen and Zhong-yu Ma, Phys. Rev. **C52**, 144 (1995).

[13] G.Q. Li and Y.Z. Zhuo, Nucl. Phys. **A568**, 745 (1994).

[14] S. Gmuca, Nucl. Phys. **A547**, 447 (1992).

[15] A. Delfino, J. Dey, M. Dey and M. Malheiro, Phys. Lett. **B363**, 17 (1995); Zeits. fur Phys.**C** (In press), hep-ph/9603403 .

[16] A. Delfino, C.T. Coelho and M. Malheiro, International Nuclear Physics Conference **(INPC'95)**, Beijing-China, August 1995, (Book of Abstract, section Mesons and Baryons in Nuclei, pg. 2-36).

[17] Z. Qian, H. Song, and R. Su, Phys.Rev.**C48**, 154 (1993).

[18] A. Bhattacharyya and S. Raha, Phys. Rev **C** (In press) and nucl-th/9603020.

[19] J. Theis, H. Stocker and J. Polony Phys. Rev. **D28**, 2286 (1993).

4 Figures and Captions

Fig. 1: Baryon effective mass in nuclear matter as a function of the temperature at $\rho = 0$.

Fig. 2: Baryon effective mass M^* as a function of the baryon density at different temperatures for the Walecka model (W) and Zimanyi-Moszkowski models (ZM, ZM2, ZM3).

Fig. 3: Proper energy/baryon as a function of baryon density at different temperatures for the Walecka model (W) and Zimanyi-Moszkowski models (ZM, ZM2, ZM3).

Fig. 4: Pressure as a function of baryon density at different temperatures for the Walecka model (W) and Zimanyi-Moszkowski models (ZM, ZM2, ZM3).

Fig. 5: Temperature as a function of the baryon density (phase diagram) for the Walecka model (W) and Zimanyi-Moszkowski models (ZM, ZM2, ZM3).

Fig. 6: Pressure as a function of baryon density at flash temperature (T_f) for the Walecka model (W) and Zimanyi-Moszkowski models (ZM, ZM2, ZM3).

Fig. 7: Entropy density as a function of baryon density at different temperatures for the Walecka model (W) and Zimanyi-Moszkowski models (ZM, ZM2, ZM3).

Table 1: Coupling constants C_σ^2 and C_ω^2; binding energy E_b (MeV) at equilibrium density $\rho_o(fm^{-3})$, m^* and the incompressibility K for the indicated models.

models	C_σ^2	C_w^2	E_b	ρ_o	m^*	K
W	357.4	273.8	-15.75	0.148	0.54	550.82
ZM	169.2	59.1	-15.90	0.160	0.85	224.71
ZM2	219.3	100.5	-15.77	0.152	0.82	198.32
ZM3	443.3	305.5	-15.76	0.149	0.72	155.74

Table 2: Values for the critical temperature T_c and the effective mass M_c^* in MeV, critical density ρ_c in fm^{-3} and pressure p_c in MeV/ fm^3 for the indicated models.

Models	T_c	ρ_c	p_c	M_c^*
Walecka	18.3	0.0650	0.4300	760
ZM	16.5	0.0698	0.2570	861
ZM2	15.5	0.0364	0.2106	881
ZM3	13.6	0.0354	0.1571	831

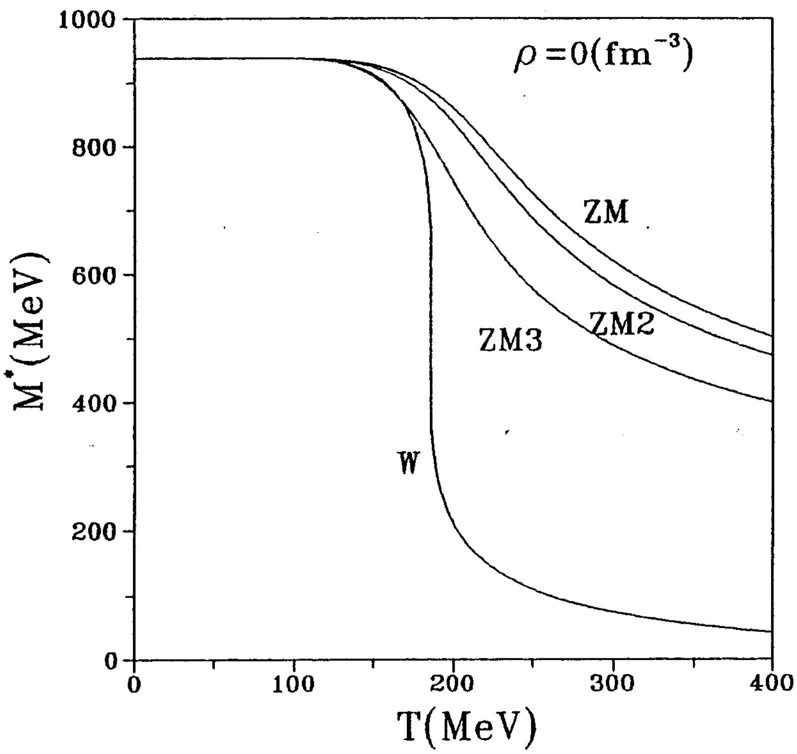

ρ=0(fm⁻³)
ZM
ZM2
ZM3
W
M*(MeV)
T(MeV)
0
200
400
600
800
1000
0
100
200
300
400

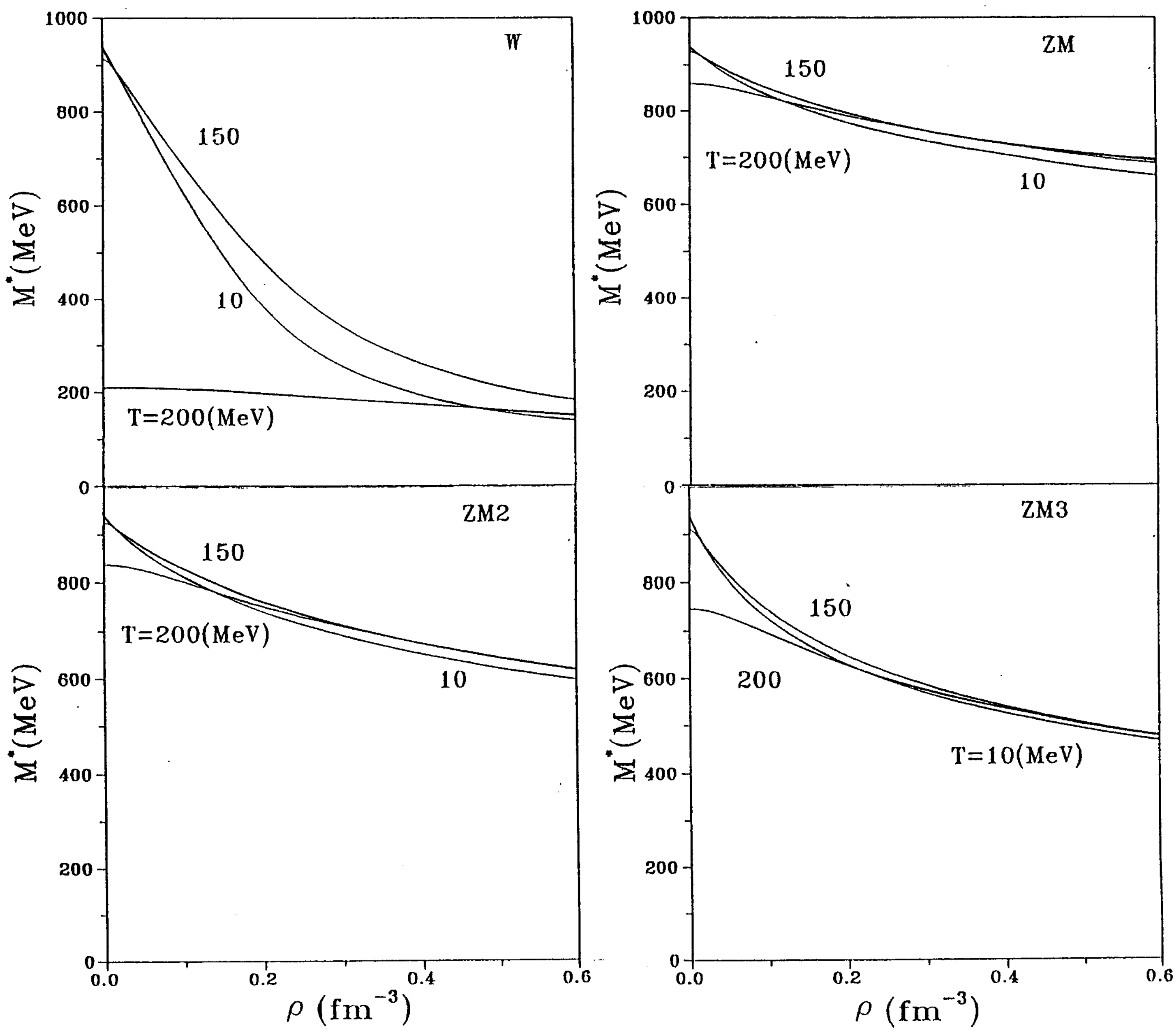

W
ZM
ZM2
ZM3
150
10
T=200(MeV)
200
T=10(MeV)
M*(MeV)
ρ (fm^-3)
0
200
400
600
800
1000
0.0
0.2
0.4
0.6

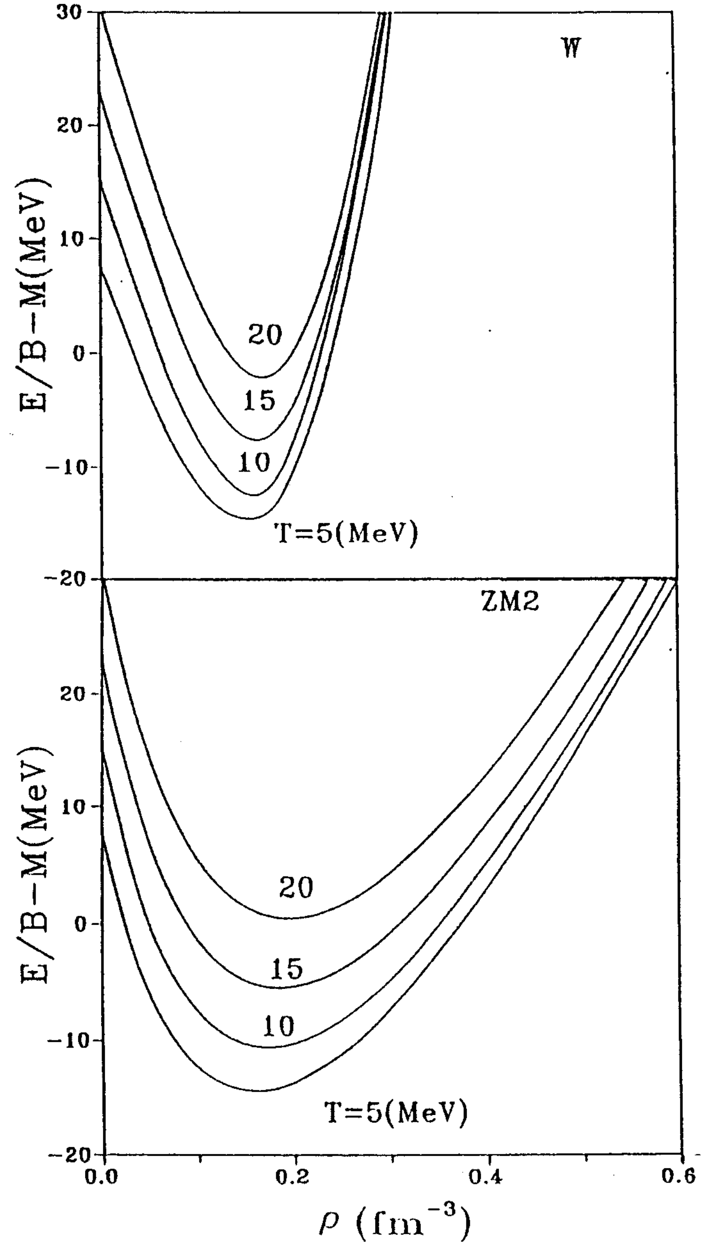

W
ZM
ZM2
ZM3
E/B−M(MeV)
ρ (fm⁻³)
20
15
10
T=5(MeV)
30
20
10
0
−10
−20
0.0
0.2
0.4
0.6

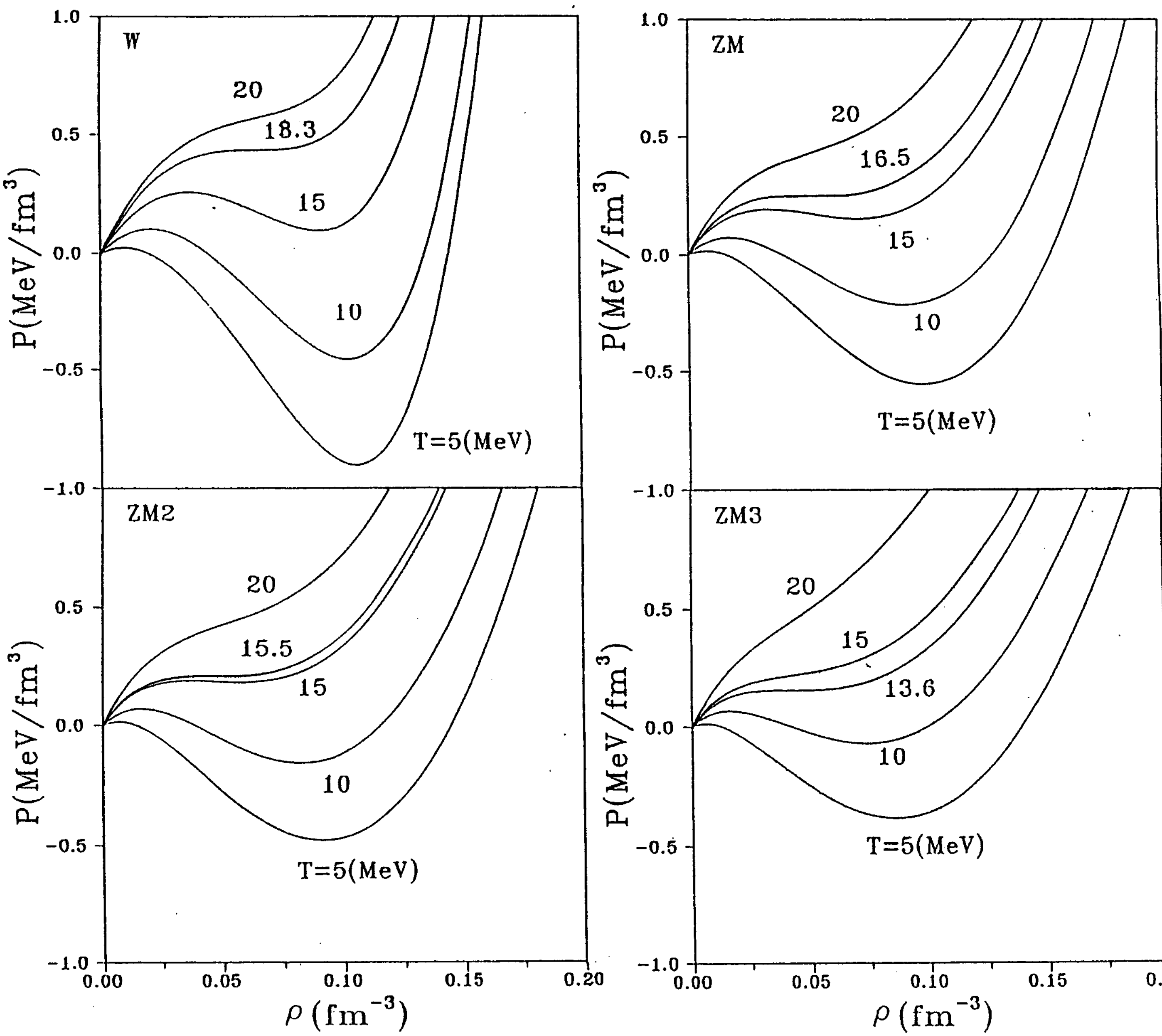

W
20
18.3
15
10
T=5(MeV)
ZM
20
16.5
15
10
T=5(MeV)
ZM2
20
15.5
15
10
T=5(MeV)
ZM3
20
15
13.6
10
T=5(MeV)
P(MeV/fm^3)
ρ (fm^{-3})
1.0
0.5
0.0
-0.5
-1.0
0.00
0.05
0.10
0.15
0.20

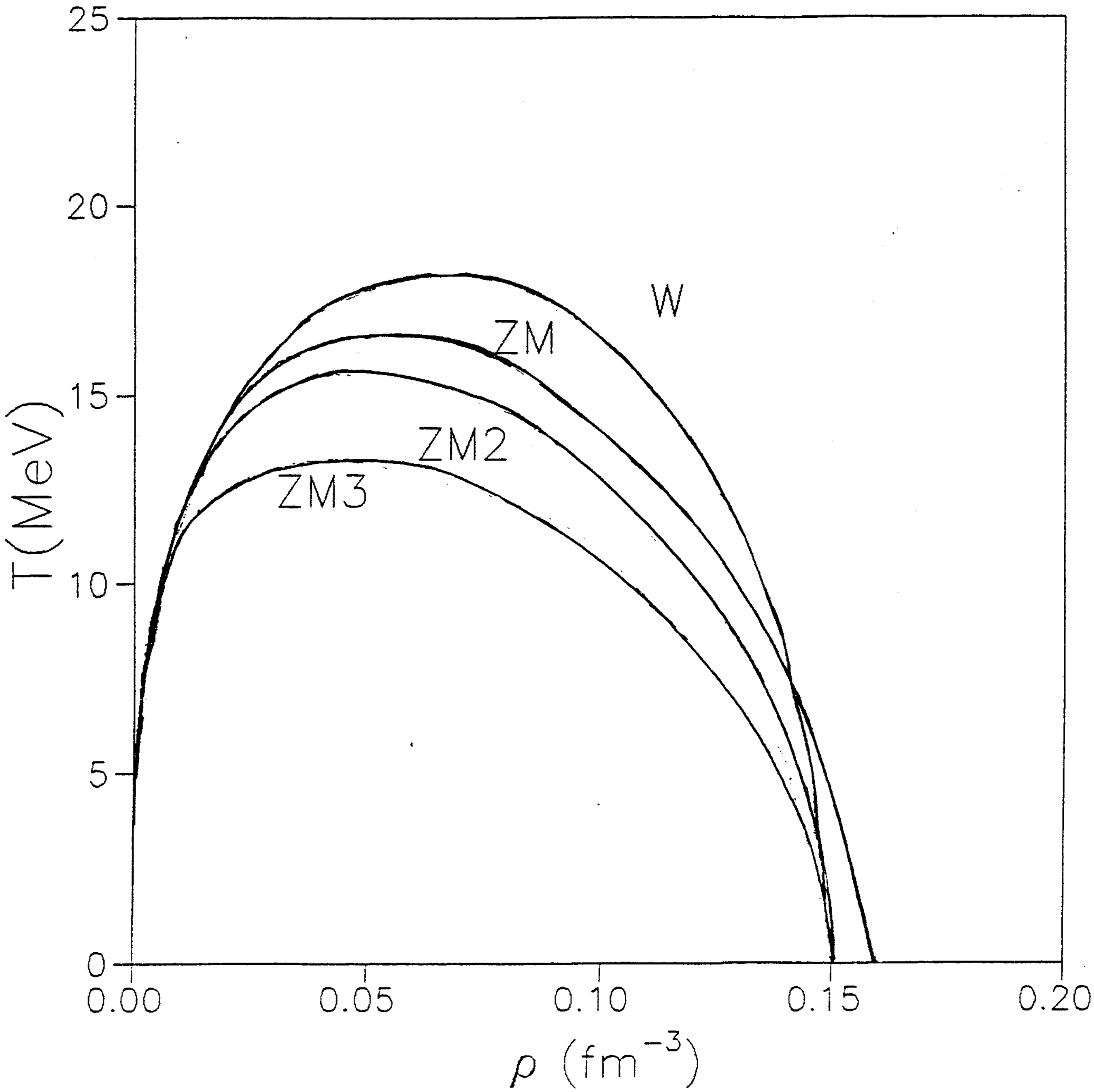

25
20
15
10
5
0
T(MeV)
W
ZM
ZM2
ZM3
0.00
0.05
0.10
0.15
0.20
ρ (fm^-3)

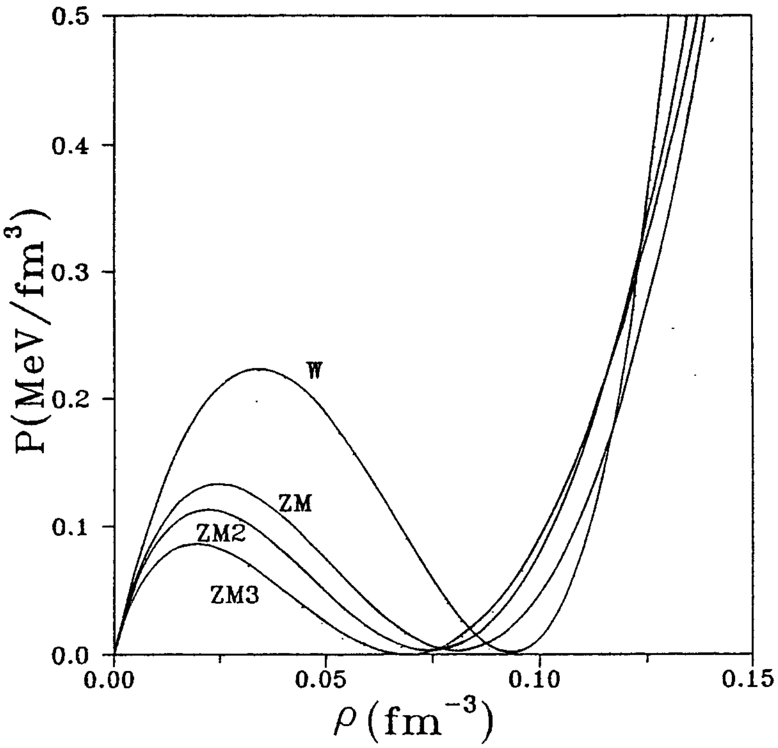

0.5
0.4
0.3
0.2
0.1
0.0
0.00
0.05
0.10
0.15
P(MeV/fm^3)
ρ (fm^{-3})
W
ZM
ZM2
ZM3

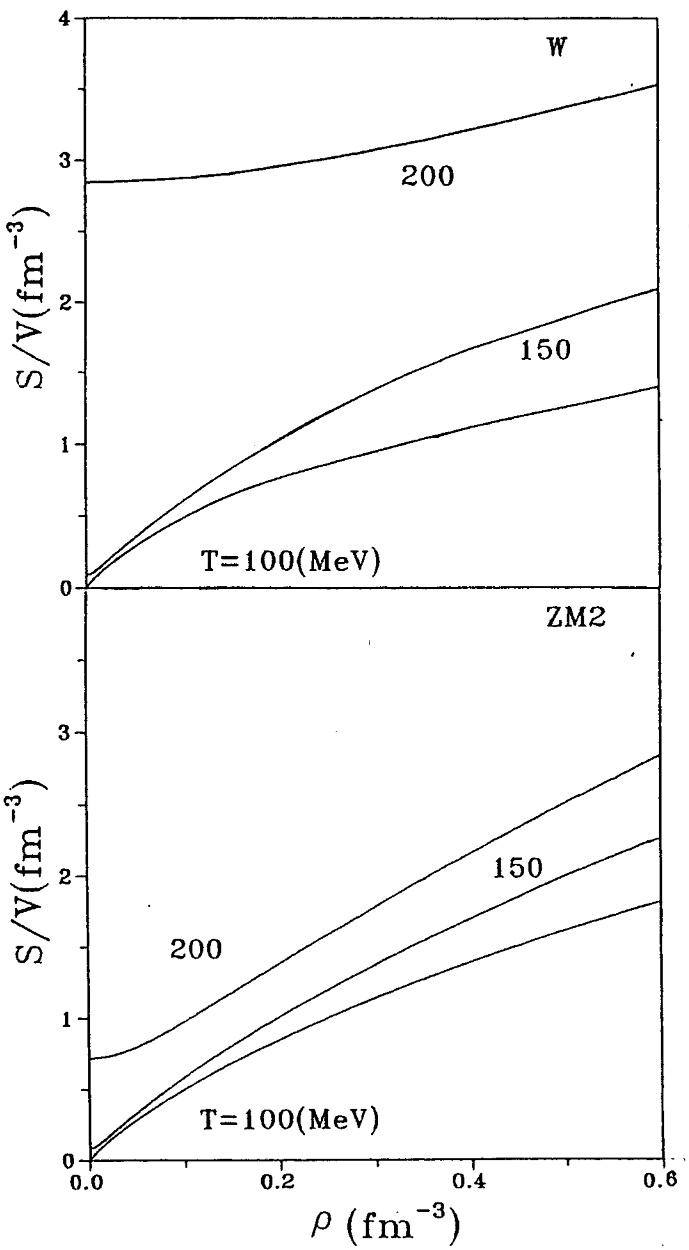

W
200
150
T=100(MeV)
ZM
200
150
T=100(MeV)
ZM2
200
150
T=100(MeV)
ZM3
200
150
T=100(MeV)
S/V(fm^-3)
ρ (fm^-3)